



NEUTRINO PHYSICS AT FERMILAB*

F. A. Nezrick

December 1977

* Invited talk at the Triangle Seminar on Recent Developments in High Energy Physics, Campione D'Italia, October 3-7, 1977.



NEUTRINO PHYSICS AT FERMILAB

F. A. Nezrick

Fermi National Accelerator Laboratory

Batavia, Illinois 60510 USA

INTRODUCTION

The scope of this report is not to survey all results from Fermilab neutrino experiments but to present to the nonspecialist the highlights of a few neutrino physics topics. The topics chosen are not necessarily the most profound of the moment but are those topics which I find interesting, namely:

1. Is the antineutrino γ -distribution energy dependent?
2. Status of dilepton production by neutrinos.
3. Properties of the hadronic system in neutrino interactions.
4. Properties of antineutrino interactions with neutrons.
5. Nuclear effects in antineutrino interactions.
6. F^+ production by neutrinos?
7. Future neutrino program at Fermilab.

The present Fermilab neutrino facility consists of two electronic detectors and the 15-ft. bubble chamber. The electronic detectors are the second generation evolution of the original Cal-Tech, Fermilab detector¹ and the Harvard, Pennsylvania, Wisconsin, Fermilab detector.² Four different neutrino beams (neglecting minor variations) are available and have been used. These beams typically operate with 400 GeV protons and intensities of $1-1.5 \times 10^{13}$ protons/pulse with a repetition rate of about 10 seconds. Figure 1 schematically illustrates the antineutrino energy spectrum of the four available beams. The horn focussed neutrino beam³ has the highest overall flux, the lowest

average energy and a strong suppression of the wrong type of neutrino (e.g., suppresses the neutrino flux in the antineutrino beam). The quadrupole triplet beam⁴ can be tuned to enhance high or low energy neutrinos but in general has a medium flux and a natural mixture of neutrinos and antineutrinos. The dichromatic beam⁵ can also be tuned to optimize different energies. The resulting neutrinos from K decays have good energy resolution (about 10%). This beam has low flux and a good suppression of wrong type neutrinos. The bare target sign selected beam⁶ (BTSS) has the lowest overall flux but most of the flux is above 50 GeV and has a very good suppression of the wrong type of neutrinos. The horn beam presently operates with a 20 μ second proton beam spill. The other beams operate with longer proton spill times typically 1 msecond or longer.

The neutrino area and detectors have been operating at Fermilab since mid-1974. The exposures given to the various detectors are outlined in Table I. Physics from the underlined exposures have not yet been reported. Most of the other experiments received substantial additional exposures during the past year and new results should be reported soon.

1. Is the Antineutrino γ -distribution Energy Dependent.

During the past few years many interesting neutrino effects have been reported; high- γ anomaly,⁷ low- γ anomaly,⁸ threshold effects in antineutrino γ -distributions,⁹ charge symmetry violation,¹⁰ a need for new exotic baryon states,¹¹ etc. Most of the above exotic effects have been dispelled. The area where an exotic effect might still exist is one aspect of the high- γ anomaly: explicitly the question is whether or not the antineutrino γ -distribution is energy dependent. Data on antineutrino γ -distributions now exist from three counter experiments and three

bubble chamber experiments and as we shall see, the answer to the question of an energy dependence is still unclear.

Consider the neutrino-nucleon interaction described by the neutrino and muon with energies E and E_μ and a virtual boson propagator carrying the energy $\nu = E - E_\mu$ and four momentum $Q^2 = 4EE_\mu \sin^2 \frac{\theta_{\mu\nu}}{2}$. The scaling variables are defined as $x = Q^2/2m\nu$ and $y = \nu/E$.

The general form of the V-A interaction is

$$\frac{d\sigma^{\nu, \bar{\nu}}}{dx dy} = \frac{G^2 ME}{\pi} \left[xF_1 y^2 + F_2(1-y) + xF_3 y(1-\frac{y}{2}) \right] \frac{1}{(1+Q^2/\Lambda^2)^2}$$

where F_i , the hadronic structure functions, are in general functions of ν and Q^2 . Assuming charge symmetry ($F_i^\nu = F_i^{\bar{\nu}}$), a very heavy propagator mass ($Q^2/\Lambda^2 \rightarrow 0$), the Callan-Gross relation ($2xF_1 = F_2$) and scaling ($F_i(\nu, Q^2) = F_i(x)$) gives:

$$\frac{d\sigma^{\nu, \bar{\nu}}}{dx dy} = \frac{G^2 ME}{\pi} \left[F_2(1-y + \frac{y^2}{2}) + xF_3 y(1 - \frac{y}{2}) \right]$$

$$\frac{d\sigma^{\nu, \bar{\nu}}}{dy} = \frac{G^2 ME}{\pi} \left[(1-y + \frac{y^2}{2}) \int F_2 dx + y(1 - \frac{y}{2}) \int xF_3 dx \right]$$

and

$$\sigma^{\nu, \bar{\nu}} = \frac{G^2 ME}{3\pi} \left[2 \int F_2 dx + \int xF_3 dx \right].$$

We introduce the infamous B parameter:

$$B = \frac{\int xF_3 dx}{\int F_2 dx}.$$

The value of B can be determined either from fitting the shape of the antineutrino y -distribution,

$$\frac{d\sigma_{\bar{\nu}}}{dy} = \frac{G^2_{ME}}{\pi} \left[(1-y+\frac{y^2}{2}) \right] - By(1-\frac{y}{2}) \int F_2 dx,$$

or from the total neutrino-antineutrino cross section ratio,

$$B = \frac{2(\sigma^{\nu} - \sigma^{\bar{\nu}})}{\sigma^{\nu} + \sigma^{\bar{\nu}}}.$$

Before looking at the data we can ask if we believe the above theoretical framework. We know that contrary to our assumptions, charge symmetry will be violated at small x because of charm production and scaling violations exist at small x . The amount of violation will increase with energy. However both of these violations are second order effects at present energies. Therefore let us use the above framework for our analysis and consider B as a parameter which describes departures of the shape of the y distribution from the simple scaling predictions. Figure 2 displays the data on the energy dependence of B for antineutrinos. The original data which "discovered" the high- y anomaly effect are from the HPWF⁷ experiment. Their B values were obtained from fitting the y distributions and show the largest energy dependence of all the data. One of the GGM¹² B values and the FIMS¹³ B values were derived from fitting the y distributions. The other GGM¹⁴ B value and the B values of CFR,¹⁵ CDHSB¹⁶ and BEBC¹⁷ were obtained from the neutrino-antineutrino cross section ratios.

In analyzing the data of Fig. 2 fits were first made assuming an energy independent B and then assuming a linear energy dependence of B . The results of these fits are given in Table II for the total data of Fig. 2, the total excluding the CDHSB data, the total excluding both CDHSB and HPWF data and for only the CDHSB data. The χ^2 per degree of freedom (χ^2/DF) is fair for the fits to the total data sample for both the energy dependent and energy independent hypothesis for B . In the overall fit the CDHSB

data are statistically overpowering. In a very high statistics experiment such as CDHSB the question of systematic biases are particularly serious. Allowing for the newness of the CDHSB data let's consider it separately. The CDHSB data taken alone shows no indication of an energy dependence. However the world data without CDHSB (with and without the HPWF data) shows a statistically significant but mild energy dependence. Therefore we observe the world data dividing itself into two groups: the CDHSB data which displays no energy dependence

$$B = (0.77 \pm 0.04) - (-1 \pm 3) \times 10^{-4} E$$

and the other five experiments which display a mild energy dependence

$$B = (0.85 \pm 0.03) - (19 \pm 4) \times 10^{-4} E$$

This experimental situation, which reminds one of the η_{00} situation of the K_L^0 of nearly 10 years ago, should be resolved within the next year or so with additional good statistics experiments being completed and continuing studies of the CDHSB data illuminating the question of possible systematic errors.

2. Status of Dilepton Production by Neutrinos

The simple quark parton model has had good success in describing¹⁸ to first order the single muon charged current interactions (Fig. 3a). Neutrino events with two leptons in the final state are usually described by the production and decay of a new particle: the leptonic decay of the intermediate vector boson (Fig. 3b), the decay of a heavy lepton (Fig. 3c) or the leptonic decay of a hadron with a new quantum number - charm (Fig. 3d). However, a normal charged current (cc) event can mimic a dilepton event if a pion forward-decays to a fast muon (Fig. 3e).

The above production mechanisms produce dileptons of opposite sign while the mimicked events produce "dilepton" signals of both opposite and the same sign. The study of dimuon production in different density targets,¹⁹ showed the pion decay background to be small in that opposite sign dimuon experiment. Dilepton final states have been studied in many counter experiments^{19,20,21} and bubble chamber neutrino experiments.^{22,23,24,25,26} I will not reference each experiment but I will give a summary of the results.

The general properties of opposite sign dileptons are:

- 1) The charged lepton associated with the incoming neutrino (i.e., the primary lepton) is on the average about six times as energetic as the second lepton.
- 2) The second lepton has a momentum distribution similar to the charged hadrons.
- 3) The transverse momentum of the second lepton is strongly correlated with the direction of the hadronic shower.

These properties rule out the intermediate vector boson decay and heavy lepton decay interpretations of dilepton production and in general support the Glashow, Iliopoulos and Maiani (GIM) four-quark model³⁰ with the new quantum number-charm. In the GIM model the second lepton comes from the decay of the charmed hadron ($D^{\pm} \rightarrow K^{\mp} \mu^{\pm} \nu$). Figure 4 gives typical quark diagrams for dilepton production from D^0 and D^+ decay from valence quark interactions and sea quark interactions. The allowed charm changing dilepton reactions are:

$$\nu + d \rightarrow \mu^- + C + \dots \quad (1)$$

$$\quad \quad \quad \downarrow$$

$$\quad \quad \quad \mu^+(e^+) + \dots$$

$$\nu + s \rightarrow \mu^- + C + \dots \quad (2)$$

$$\quad \quad \quad \downarrow$$

$$\quad \quad \quad \mu^+(e^+) + \dots$$

$$\bar{\nu} + \bar{s} \rightarrow \mu^+ + \bar{C} + \dots \quad (3)$$

$$\quad \quad \quad \downarrow$$

$$\quad \quad \quad \mu^-(e^-) + \dots$$

$$\bar{\nu} + \bar{d} \rightarrow \mu^+ + \bar{C} + \dots \quad (4)$$

$$\quad \quad \quad \downarrow$$

$$\quad \quad \quad \mu^-(e^-) + \dots$$

where the D^+ (D^0) is a $c\bar{d}$ ($c\bar{u}$) state. The rates for reactions (1), (2) and (3) are comparable since reaction (1) is with a valence quark but suppressed by $\sin^2 \theta_c$ (5%). Reactions (2) and (3) are only suppressed by the fraction of momentum carried by the sea quarks relative to the valence quarks (~4%). Reaction (4) is negligible since it is suppressed by both factors. Since the total antineutrino to neutrino charged current cross section is 0.5, the relative yield of dilepton to single lepton events should be about the same for neutrinos and antineutrinos. Figure 5 gives the dilepton to single lepton cross section ratio as a function of neutrino energy for $\mu\mu$ and μe final states for neutrino and antineutrino interactions. There is reasonably good agreement with the GIM model.

As seen in Fig. 4 the charmed meson decay always produces a neutral or charged K meson. In addition a second K meson is produced if the interaction is off a strange quark. Assuming the GIM model, every dilepton should have at least one associated K meson. No experiment to date has had decent efficiency for detecting charged K mesons. The bubble chamber experiments have high efficiency for detecting $K_S^0 \rightarrow \pi^+\pi^-$ thereby providing a good test of the

GIM model. Assuming the rate for associated production of strange particles in dilepton events is the same as in single lepton events, the GIM model predicts a K^0 multiplicity of 0.8 per dilepton event.³¹ The relative rate for events containing at least one neutral strange particle (K_S^0 , Λ) in single lepton events^{32,33} is only 0.14. Table III lists the present status of bubble chamber results on the K^0 rate in dilepton events. Experimental results exist only for neutrino interactions. Three experiments agree with the GIM prediction while the other two disagree with the prediction. Except for the experimentally unclear K^0 rate, all the data on opposite sign dileptons are in substantial agreement with the GIM model.

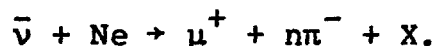
Exotic dilepton events have been reported where both leptons have the same sign.³⁴ Experimentally the same sign dimuon sample has a large background from π and K decays (Fig. 3e). From the rate in different density targets it appears that the same sign dimuon signal is probably real and the rate for same sign dimuons is about 10% of the opposite sign dimuon rate. What could be the source of the same sign dimuon events? To illustrate the richness of possible production mechanisms let us introduce charm, the neutral heavy lepton (M^0) the charged heavy lepton (M^\pm), the top quark (t) and the bottom quark (b). Consider the following possible dimuon production mechanisms. Charm-anticharm pair production at the hadronic vertex when one decays via an electron and the other via a muon (Fig. 6a). Since the electronic detectors cannot observe the electron these events would be classified as same sign dimuon events. The cascade decay of a charged heavy lepton (Fig. 6b) results in same sign dimuon events with both muons of high momentum. A neutral current interaction producing a neutral heavy lepton and a bottom quark (Fig. 6c) also would result in same sign dimuon events. To firmly establish the same sign dilepton effect we must await clean higher statistics experiments.

Also needed are new (bubble chamber) experiments to determine the extent of $\mu\mu e$ production to determine the source of the same sign dilepton events.

3. Properties of Hadrons in Neutrino Interactions

The early studies of neutrino interactions with protons³⁵ showed that the mean charged hadronic multiplicity is a function only of the mass (W) of the hadronic system. Comparisons of the mean charged multiplicity in νp , νe , νp and νp interactions indicate only a dependence on the mass of the excited state, see Fig. 7, and no dependence on the type of incident particle. Comparisons of electron neutrino and pion interactions in neon indicate similar dependences, see Fig. 8.

Preliminary studies of inclusive π^- production are presented here³⁶ for the reaction



In the bubble chamber it is difficult, except at low momentum, to distinguish between a proton and π^+ meson. The positive tracks therefore contain mesons and baryons. The π^- studies do not suffer from baryon contamination. Figure 9 gives the comparison of the mean multiplicity of π^- for $\bar{\nu}$ -Ne and π^-d for the hadronic mass squared region of 4 to 100 GeV^2 . Again the agreement is good.

Figure 10a compares the invariant yield³⁸ of π^- as a function of the Feynman x variable for $\bar{\nu}$ -Neon and $\bar{\nu}$ -proton³⁹ interactions. These distributions have been normalized to the same area. The excellent agreement allows the following conclusions:

- 1) There is no large difference in the shape of the π^- invariant yield distribution for anti-neutrino-neutron interactions and antineutrino-proton interactions.
- 2) Nuclear effects, final state interactions, etc., in the neon data do not produce substantial changes in the shape of the π^- invariant yield distribution.

In Fig. 10b the invariant π^- yield for $20 < w^2 < 100 \text{ GeV}^2$ is compared with that from π^-p and π^-n interactions⁴⁰ in the same hadronic mass range, $s \approx 35 \text{ GeV}^2$. The distributions which have been normalized to the same area in the region $-0.4 < X_F < 0.4$ agree very well in shape except for the characteristic forward peak (leading particle effect) in the hadron data which is not present in the antineutrino data.

In all studies to date the properties of the hadronic system in neutrino interactions, charged lepton, pion and nucleon interaction exhibit similar behaviors.

4. Properties of Antineutrino Interactions with Neutrons

Preliminary results have been presented recently⁴¹ on extracting from the $\bar{\nu}$ -neon bubble chamber data the $\bar{\nu}$ -neutron to $\bar{\nu}$ -proton cross section ratio and the relative shapes of the inclusive x and y distributions for charged current interactions. The best way to study interactions with neutrons is by using deuterium targets. However high energy neutrino-deuterium experiments will not start until mid-1978. The neutron data extracted from interactions with neon gives us an early look. These results are preliminary. Since events with only one charged track in the final state were not recorded, the $\bar{\nu}$ -proton sample could be underestimated.

Antineutrino interactions with free neutrons produce final states with charge zero while interactions with free protons produce final states with charge plus one. Interactions with bound nucleons produce final states with the same respective charges except for charge shifts due to final state interactions, etc. Final state charge shifts were shown to be independent of the dynamics of the event to first order (E, W, Q^2 etc.). The following procedure is therefore used to separate the neutron and proton events:

Let:

- N_0 = Number of true $\bar{\nu}$ -neutron charged current events off Neon.
 N_1 = Number of true $\bar{\nu}$ -proton charged current events off Neon.
 N_{H2} = Number of true $\bar{\nu}$ -proton charged current events off H_2 .
 N_j^* = Number of observed events with charge j .
 W_k = Probability of a change of true final state charge by K units.

Then:

	Number of Events Observed with Charge N_j^*
$N_{-1}^* = N_0 W_{-1} + N_1 W_{-2}$	5
$N_0^* = N_0 W_0 + N_1 W_{-1}$	110
$N_1^* = N_0 W_1 + N_1 W_0 + N_{H2} W_0$	378
$N_2^* = N_0 W_2 + N_1 W_1$	109
$N_3^* = N_0 W_3 + N_1 W_2$	45
$N_4^* = N_0 W_4 + N_1 W_3$	10
$N_5^* = N_0 W_5 + N_1 W_4$	7

Using the overall constraint that $\sum W_i = 1$ and neglecting transitions of order W_{-2} and W_5 we solve the above set of equations for

$$1) \quad \frac{N_0}{N_1} = \frac{\sigma(\bar{\nu}n)}{\sigma(\bar{\nu}p)}$$

2) $N_1 W_{-1}$: the proton contamination in the neutron sample

3) $N_0 (W_1 + W_2 + W_3 + W_4)$: the neutron contamination of the proton sample.

The solution gives:

$$1) \quad \frac{\sigma(\bar{\nu}n)}{\sigma(\bar{\nu}p)} = 0.51 \pm 0.07$$

2) The neutron sample is 8% contaminated by proton events.

3) The proton sample is 10% contaminated by neutron events.

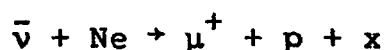
The neutron-proton cross section ratio is consistent with the quark-parton model prediction ($d\bar{d}u/u\bar{u}d$) of 0.50. Since the neutron-proton cross contamination is small (1 and 2 above) one can select neutron events as those with observed charges zero and minus one and proton events as all other final charged states (accepting the 10% contamination). The resulting cross section ratio as a function of x and y are shown on Fig. 11 and are compared with the predictions of Field and Feynman.⁴² The theoretical predictions agree very well with the data including the dramatic variation with x .

5. Nuclear Effects in Antineutrino Interactions

In the previous section it was shown that nuclear

effects did not produce large changes in the average multiplicities or in the shape of the inclusive invariant yield of negative particles (Figures 9, and 10). Nuclear effects in hadron interactions, although small, have been studied by investigating the properties of particles produced in kinematic regions forbidden to free nucleon interactions. This forbidden region is usually taken as protons emitted in the backward hemisphere in the laboratory. The original studies of nuclear effects done in the USSR^{3,4} demonstrated that; (1) the slope of the momentum spectrum of backward emitted protons is independent of incident particle type and momentum, (2) the slope is a function of the laboratory angle of the backward protons, (3) the yield of high energy backward particles is substantially larger (by more than 100) than expected from Fermi motion, (4) the momentum of backward protons is higher than usually expected from Fermi motion. Present theoretical interpretations of this effect include cumulative effects,⁵ nuclear scaling,⁶ nucleon pair correlations,⁷ quasi two-body scaling,⁸ etc.

Preliminary results are reported here on the reaction



where the proton is emitted in the backward hemisphere. Protons were selected by range-momentum for positive tracks stopping in the bubble chamber. This required the proton momentum to be between 0.2 GeV/c and 0.7 GeV/c. In a sample of 830 charged current events with total energy above 10 GeV, 35 events had identified backward protons in the above momentum range. The momentum spectrum of the backward protons was fit to the functional form used in the earlier hadronic experiments;

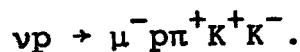
$$\frac{E}{p^2} \frac{dN}{dp} = C e^{-Bp^2}$$

where E is the neutrino energy and p is the proton momentum, giving $B = 9 \pm 2$. The fit and the data are given in Fig. 12. This fitted B value agrees well with those found in the hadronic experiments, see Fig. 13.

Further studies are continuing to understand the differences between the backward proton events and the normal charged current event. With increased statistics these differences can help to isolate the production mechanism for nuclear events.

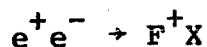
6. F⁺ Production by Neutrinos?

In the neutrino-hydrogen bubble chamber experiment new results have been reported⁴⁹ on well constrained kinematic fits. This new data sample contains about 2,000 charged current events. Five events make good 3-constraint fits to the reaction



The invariant mass of the $(K^+ K^- \pi^+)$ combinations are 1361 ± 3 MeV, 1583 ± 3 MeV, 1716 ± 4 MeV, 2038 ± 4 MeV and 2321 ± 7 MeV. The K^- in the 2038 MeV event is uniquely identified since it decays and has a good kinematic fit for the decay $K^- \rightarrow \mu^- \nu$.

Results from colliding beam experiments indicate



with an F^+ mass of 2030 ± 60 MeV from DESY.⁵⁰ The neutrino event with a mass $M(K^+ K^- \pi^+)$ of 2038 ± 4 MeV could be an indication of F^+ production.

7. Future Neutrino Program at Fermilab

The Fermilab neutrino facility has matured in its reliability and with new improvements has shown substantially versatility in the past year. The high points of the future neutrino program at Fermilab will be presented including new neutrino beams, improved detectors, deuterium targets, and a future 1 TeV neutrino facility.

a. Present Neutrino Facility Improvements and Schedule

A new dichromatic beam⁵² (NDB) for neutrinos and anti-neutrinos has been constructed. This beam will (1) allow mesons of up to ~350 GeV to be focussed; (2) have a greatly suppressed wide-band background, (3) have an improved momentum dispersion at higher energies and (4) have the possibility of operating at even higher secondary energies (up to ~425 GeV) if Fermilab operates in the energy doubler mode.⁵³ A dichromatic horn beam⁵⁴ DHB is also being constructed.⁵⁵ This beam is designed to operate at lower secondary momenta 50 to 150 GeV/c where the NDB has substantial acceptance limitations. The momentum resolution of the DHB and the NDB are comparable. The wide-band background in the DHB is worse than in the NDB but still acceptable. An overall event rate of 0.1-0.2 events per picture is possible in the neon filled 15-foot chamber running at 10^{13} protons per pulse using the DHB. The horn beams have been operated in the past with a 20 μ second spill length. In early 1978 they will be modified to operate with a spill length of ~1 msec.⁵⁶

The electronic detectors are being substantially modified. The original HPWF detector has been modified⁶⁴ to have (1) a variable density target region, (2) wide gap optical spark chambers throughout the target region, (3)

muon spectrometer of better acceptance - the 4 m diameter magnetic spectrometer is replaced by an 8 m diameter spectrometer and (4) better momentum resolution on high energy muon tracks. The original CF detector is being modified to have (1) several different density targets with approximately the same muon acceptance for the different targets, (2) increased target mass, (3) improved event position information in the target region, (4) a muon spectrometer with larger angular acceptance and better muon momentum determination.

The external muon identifier behind the 15-foot bubble chamber has been substantially improved to give a higher degree of confidence in muon identification. These improvements include a second plane of proportional wire chambers, a prototype picket fence detector⁵⁷ to time the neutrino event, and improved chamber hit and data storage systems.

Enough deuterium is now available so that the 15-foot chamber can be operated with a complete deuterium filling. The deuterium will come from the USA deuterium pool which includes Argonne National Laboratory and Brookhaven National Laboratory.

A thin multiplate system has been developed for the 15-foot bubble chamber (see Fig. 14). The plate system was designed to give; (1) a high probability of intercepting and converting γ -rays, (2) a high probability of identifying electrons from the primary neutrino vertex and (3) allow the momentum and direction of the converted γ -rays to be determined well enough to do analysis of reactions including a single π^0 in the final state.

A tentative schedule for the neutrino facility for 1978 is given in Table IV where C1 and C2 are the upgraded detectors of the HPWF and CF collaborations. If the plate testing is successful in March then the D_2 running of the bubble chamber could be with plates. It is expected that

the counter experiment and the bubble chamber would operate together in the new narrow-band beam.

b. Plans for a 1 TeV Neutrino Facility

The next generation of neutrino physics at Fermilab is centered around the accelerator operating at 1 TeV. It is expected that the Tevatron will be operating around 1980. The present plans include improvements in the neutrino facility and detectors.

The muon shield will be strengthened so that the neutrino beams can operate at full energy. It is planned that the muon and hadron beams be removed from the muon shield of the neutrino beam thus allowing the muon shield to be more homogeneous. It is hoped that a muon flux measuring system will be built in the muon shield so that the absolute neutrino flux can be determined.

The next generation of neutrino counter experiments^{58, 59, 60} are under active design and prototype testing. The main thrust of these new detectors will be (1) to detect the direction and magnitude of the energy flow in neutrino interactions, (2) identify electrons, (3) have high mass to look for "rare" processes and (4) have fine granularity (special resolution) in the target-calorimeter region.

It is proposed by some physicists that the 15-foot bubble chamber be developed into a detector which will give more complete information for each neutrino event. The neutrino event rate using the Tevatron will be lower per day per unit mass than at present at Fermilab. Therefore maximum information should be extracted from each neutrino event. These ideas are still in an embryo stage but are following the general trend of the development of the 30-inch bubble chamber External Particle Identifier

(EPI) at Fermilab,⁶¹ the BEBC EPI at CERN⁶² and the early suggestion for an "Ω" type detector for neutrino physics.⁶³

In the ideal detector one desires for each event;

- (1) the possibility of the interaction on a simple target (H_2 or D_2).
- (2) the momentum and direction of each outgoing track,
- (3) the identification of each track (is it a π , K , μ , e ...)
- (4) a measurement of the energy flow for the neutral particles and
- (5) good detection efficiency for neutral strange particles.

Figure 15 schematically illustrates the original⁶³ general arrangement of a bubble chamber hybrid detector which achieves the above goals. The present challenge is in trying to match these ideal desires with the existing bubble chamber.

REFERENCES

- ¹B. Barish, et al., Phys. Rev. Lett. 31, 565 (1973).
- ²A. Benvenuti, et al., Phys. Rev. Lett. 30, 1084 (1973).
- ³F. A. Nezrick, Nucl. Science, Vol. NS-22, No. 3, 1479 (1975).
- ⁴A. Skuja, et al., Fermilab Report TM-469 (1974).
- ⁵P. Limon, et al., Nucl. Instrum. Methods, 116, 317 (1974).
- ⁶R. Stefanski and H. B. White, Fermilab Report TM-626A (1976).
- ⁷A. Benvenuti, et al., Phys. Rev. Lett. 36, 1478 (1976).
- ⁸See for example, F. Sciulli, Proceedings of Neutrino '75 Conference, Balatonfured, Hungary (1975).
- ⁹A. Benvenuti, et al., Phys. Rev. Lett. 37, 189 (1976), and Ref. 7.
- ¹⁰B. Aubert, et al., Phys. Rev. Lett. 33, 984 (1974) and A. Benvenuti, et al., Proceedings of International Neutrino Conference, Aachen, (1976).
- ¹¹A. Benvenuti, et al., Phys. Rev. Lett. 37, 1095 (1976).
- ¹²D. H. Perkins, Proceedings of Symposium on Lepton and Photon Interactions, Stanford University (1975).
- ¹³Fermilab-IHEP-ITEP-Michigan Neutrino Group, Phys. Rev. Lett. 39, 382 (1977).
- ¹⁴W. Krenz, Proceedings of International Neutrino Conference, Aachen, (1976).
- ¹⁵B. C. Barish, et al., Phys. Rev. Lett. 38, 314 (1976).
- ¹⁶M. Holder, et al., Phys. Rev. Lett. 39, 433 (1977).
- ¹⁷P. C. Bosetti, et al., Phys. Lett. 70B, 273 (1977).
- ¹⁸See for example, E. A. Paschos, Proceedings of International Neutrino Conference, Aachen (1976).
- ¹⁹A. Benvenuti, et al., Phys. Rev. Lett. 35, 1199 (1975).

- ²⁰B. C. Barish, et al., Phys. Rev. Lett. 36, 939 (1976)
and B. C. Barish, et al., Phys. Rev. Lett. 39, 981 (1977).
- ²¹M. Holder, et al., Phys. Lett. 69B, 377 (1977).
- ²²P. Bosetti, et al., Phys. Rev. Lett. 38, 1248 (1977).
- ²³J. P. Berge, et al., Phys. Rev. Lett. 38, 266 (1977).
- ²⁴C. Baltay, et al., Phys. Rev. Lett. 39, 62 (1977).
- ²⁵H. H. Bingham, Proceedings of International Neutrino
Conference, Elbrus, USSR (1977).
- ²⁶C. T. Murphy Proceedings XIIth Rencontre de Moriond,
(1977).
- ²⁷D. C. Cundy, Proceedings of International Neutrino Con-
ference, Elbrus, USSR (1977).
- ²⁸W. Venus, Proceedings of International Symposium on
Lepton and Photon Interactions at High Energies, Ham-
burg (1977).
- ²⁹H. Deden, et al., Phys. Lett. 67B, 474 (1977).
- ³⁰S. L. Glashow, et al., Phys. Rev. D2, 1285 (1970).
- ³¹M. K. Gaillard, Proceedings of International Neutrino
Conference, Aachen, (1976).
- ³²J. P. Berge, et al., Phys. Rev. Lett. 36, 127 (1976).
- ³³J. von Krogh, Proceedings of International Neutrino
Conference, Aachen (1976).
- ³⁴A. Benvenuti, et al., Phys. Rev. Lett. 35, 1199 (1975)
- ³⁵J. W. Chapman, et al., Phys. Rev. Lett. 36, 124 (1976).
- ³⁶I wish to thank the Fermilab-U. of Michigan - ITEP,
Moscow-IHEP, Serpukhov neutrino group for allowing me
to present these preliminary data.
- ³⁷H. J. Lubatti, Proceedings of International Neutrino
Conference, Elbrus, USSR (1977)
- ³⁸The invariant yield as a function of Feynman x is
defined

$$f(x_F) \propto \int_{\bar{W}}^{E^*} \frac{d^2\sigma}{dx_F dP_t^2} dP_t^2$$

where E^* is the π^- energy in the hadronic rest frame, P_l and P_t is the longitudinal and transverse momentum of the π^- relative to the direction of the W^- and $x_F = 2P_l/W$.

- ³⁹M. Derrick, et al., submitted to Phys. Rev. D.
- ⁴⁰J. Beaupre, et al., Phys. Lett. 37B, 432 (1971) and W. D. Shephard, et al., Phys. Rev. Lett. 27, 1164 (1971).
- ⁴¹S. Kruchinin, Proceedings of International Neutrino Conference, Elbrus, USSR (1977).
- ⁴²R. D. Field and R. P. Feynman, Caltech Preprint CALT-68-565 (1977).
- ⁴³Yu. D. Bayukov, et al., Sov. J. Nucl. Phys. 18, 639 (1974).
- ⁴⁴A. M. Baldin, et al., Sov. J. Nucl. Phys. 18, 41 (1974).
- ⁴⁵A. M. Baldin, JINR Preprint E2-9138 (1975).
- ⁴⁶G. A. Leksin, Elementarnie Chastitci. 2, 5 (1977) and G. A. Leksin, Proceedings of XVIII International Conference on High Energy Physics, Tblisi, USSR (1976).
- ⁴⁷L. L. Frankfurt and M. I. Strikman, Phys. Lett. 69B, 93 (1977).
- ⁴⁸S. Frankel, Phys. Rev. Lett. 38, 1338 (1977).
- ⁴⁹G. Lynch, Proceedings of Particles and Fields Meetings, Argonne (1977).
- ⁵⁰R. W. Brandelik, et al., Phys. Lett. 70B, 132 (1977).
- ⁵²D. A. Edwards and F. J. Sciulli, Fermilab Report TM-660 (1976).
- ⁵³R. R. Wilson, Physics Today 30, No. 10, 23 (1977).
- ⁵⁴F. A. Nezrick, Nuclear Science, Vol. NS-18, No. 3, 759 (1971).
- ⁵⁵C. Baltay and D. Cohen, Proposal to Fermilab (1974).
- ⁵⁶F. A. Nezrick, Fermilab Report TM-536 (1974).
- ⁵⁷M. L. Stevenson, LBL Physics Note 809 (Oct., 1975).
- ⁵⁸J. K. Walker, Fermilab Proposal No. 563 (1977).
- ⁵⁹A. L. Sessoms, Fermilab Proposal No. 541 (1977).
- ⁶⁰H. H. Chen, Fermilab Proposal No. 496 (1977).

- ⁶¹I. A. Pless, Fermilab Proposal No. 570 (1977).
- ⁶²M. Aderholz, et al., Nucl. Instr. and Meth., 123, 237 (1975).
- ⁶³W. Venus and H. Wachsmuth, CERN Report TCL/Int. 75-3 (1975).
- ⁶⁴See for example, A. Benvenuti, et al., Phys. Rev. Lett. 38, 1110 (1977).

TABLE I
NEUTRINO EXPOSURES AT FERMILAB SINCE 1974

Beam → Detector ↓	Horn	Quad Triplet	Dichromatic	BTSS
CF and variants			$\nu, \bar{\nu}$	
HPWF and variants	$\nu, \bar{\nu}$	$\nu + \bar{\nu}$		$\bar{\nu}$
15' chamber H ₂	$\nu, \bar{\nu}$			
15' chamber H ₂ -Ne (21%)	$\nu, \bar{\nu}$			
15' chamber H ₂ -Ne (>50%)	$\nu, \bar{\nu}$	<u>$\nu + \bar{\nu}$</u>		<u>$\bar{\nu}$</u>

Underlined exposures not yet reported.

TABLE II

FITS TO $B = B_0 - E\Delta B$ AND $B = B'_0$ FOR DATA ON FIG. 2

Data Set	B_0	ΔB ($\times 10^{-4}$)	χ^2/DF	B'_0	χ^2/DF
Total Data	0.81 ± 0.025	5 ± 2	33/31	0.775 ± 0.013	37/32
Total minus CDHSB	0.85 ± 0.032	19 ± 4	12/14	0.765 ± 0.025	28/15
Total minus CDHSB minus HPWF	0.84 ± 0.035	16 ± 4	6.3/12	0.765 ± 0.025	17/13
CDHSB	0.77 ± 0.04	-1 ± 3	8.8/15	0.775 ± 0.017	9/16

TABLE III
 SUMMARY OF K^0 MULTIPLICITY IN NEUTRINO
 PRODUCED DILEPTON EVENTS

Experiment		$\frac{\mu \ell K^0}{\mu \ell}$	ℓ
WBHC ²²	ν -15' B.C.	$1.8^{+0.7}_{-0.5}$	e^+
CB ²⁴	ν -15' B.C.	0.6 ± 0.2	e^+
BBBERSU ²⁶	ν -BEBC	0.8 ± 0.5	e^+
ABCLOS ²⁷	ν -BEBC	$1.7^{+0.7}_{-0.6}$	$e^+ + \mu^+$

TABLE IV
TENTATIVE FERMILAB NEUTRINO PROGRAM FOR 1978

<u>When</u>	<u>Neutrino Beam</u>	<u>Counter Experiment</u>	<u>Bubble Chamber</u>
Oct. 1977 ↓ Feb. 1978	Quadrupole Triplet Beam ($\nu + \bar{\nu}$)	C ₁ Run	Run H-Ne
March ↓ July ↓ Oct. ↓ Dec. 1978	NDB Tests Wide-Band Horn Beam ($\nu, \bar{\nu}$) NDB ($\nu, \bar{\nu}$)	C ₂ Testing ? C ₂ Run	Plate Tests Run D ₂ (Plates) Run H-Ne

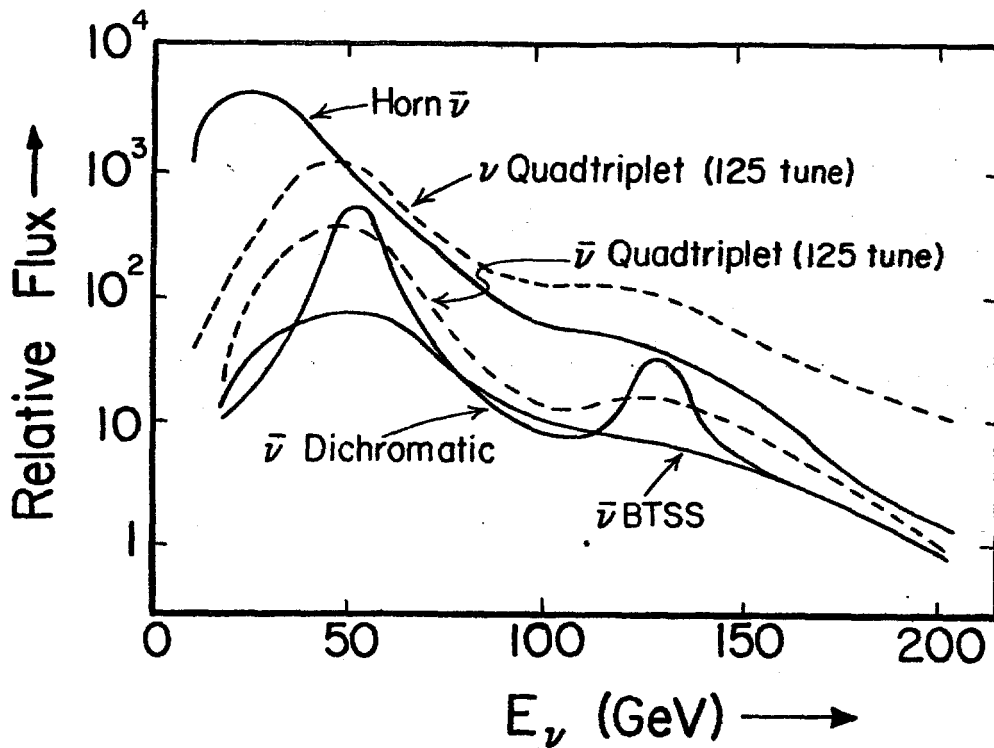


Figure 1

Antineutrino flux from the four different beams available at Fermilab. The flux distributions for the horn focussed beam,³ the dichromatic beam⁵ and the bare target sign selected (BTSS) beam⁶ are for the beams focussing antineutrinos and defocussing neutrinos. The quadrupole triplet beam⁴ focusses neutrinos and antineutrinos together with the shown flux distributions for the 125 GeV tune.

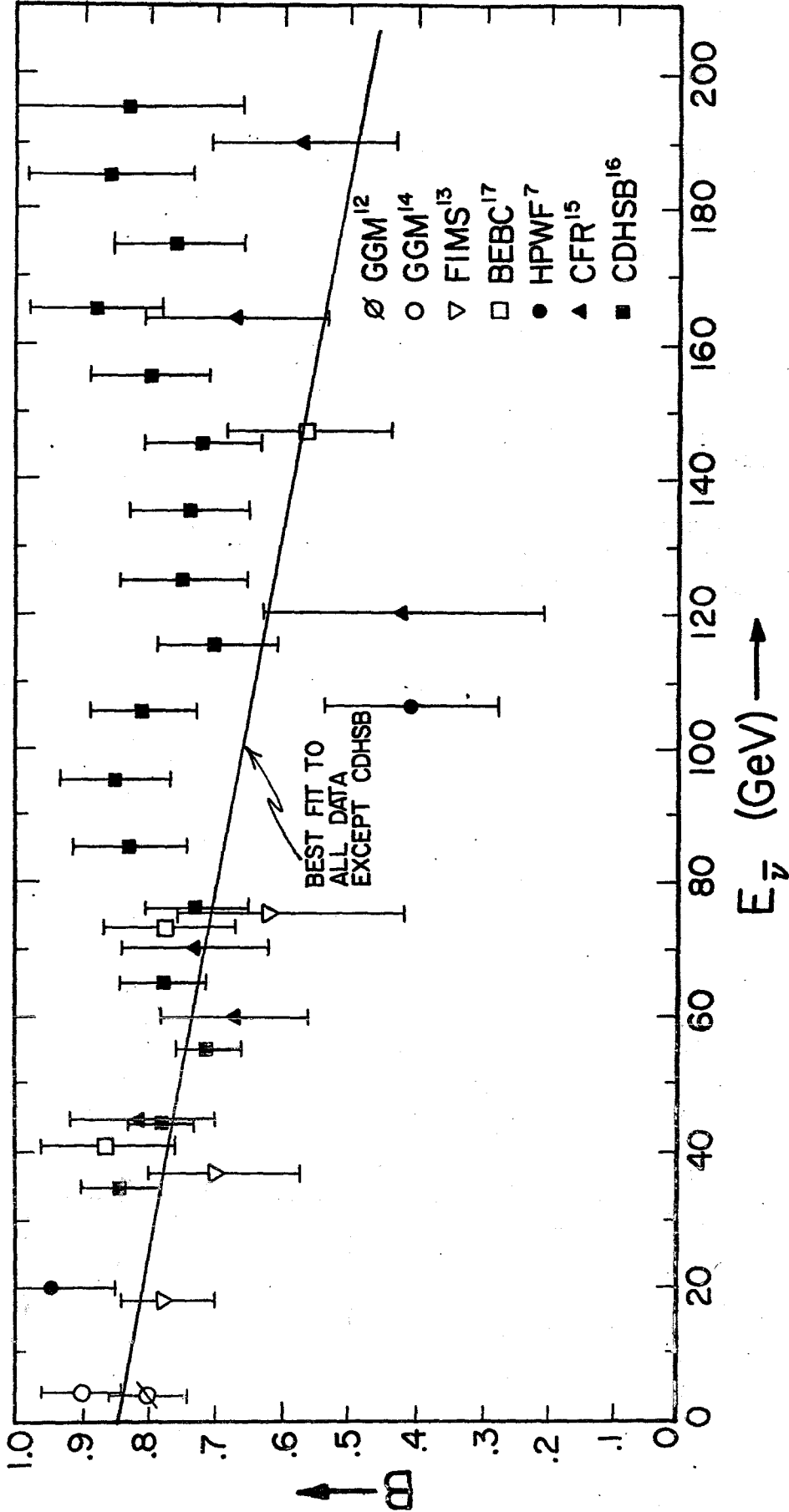


Figure 2

B values as a function of antineutrino energy. The data are plotted at the mean of the energy intervals. The black data points are from counter experiments, the open data points are from bubble chamber experiments. Solid line is a linear least squares fit to all data excluding CDHSB (see text).

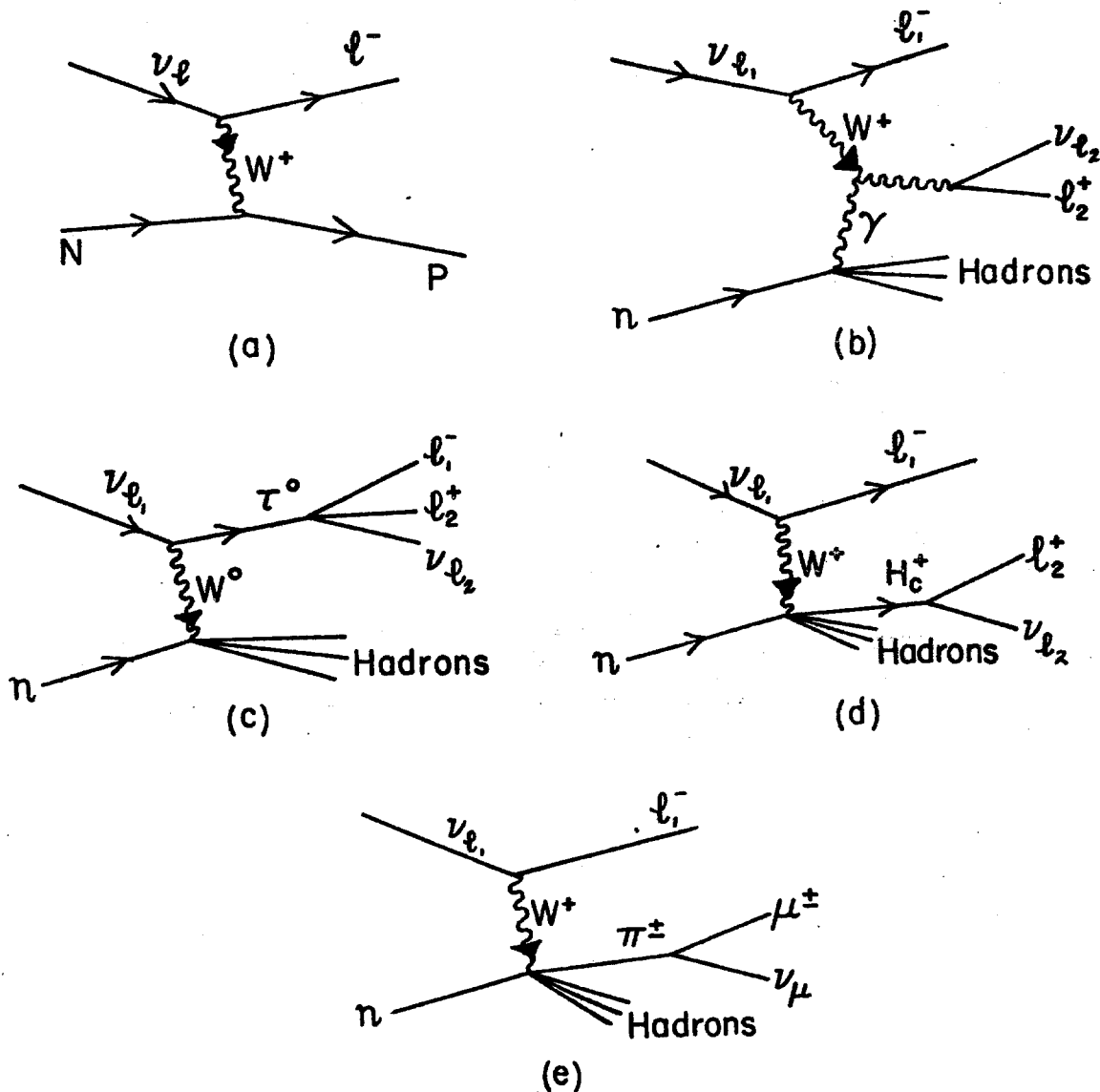


Figure 3

Production mechanisms for dilepton events. The charged current reaction (a), can have two leptons in the final state resulting from the decay of an intermediate vector boson W^+ (b), a heavy lepton τ^0 (c), charmed hadron H_c^+ (d), or normal pion decay in flight (e).

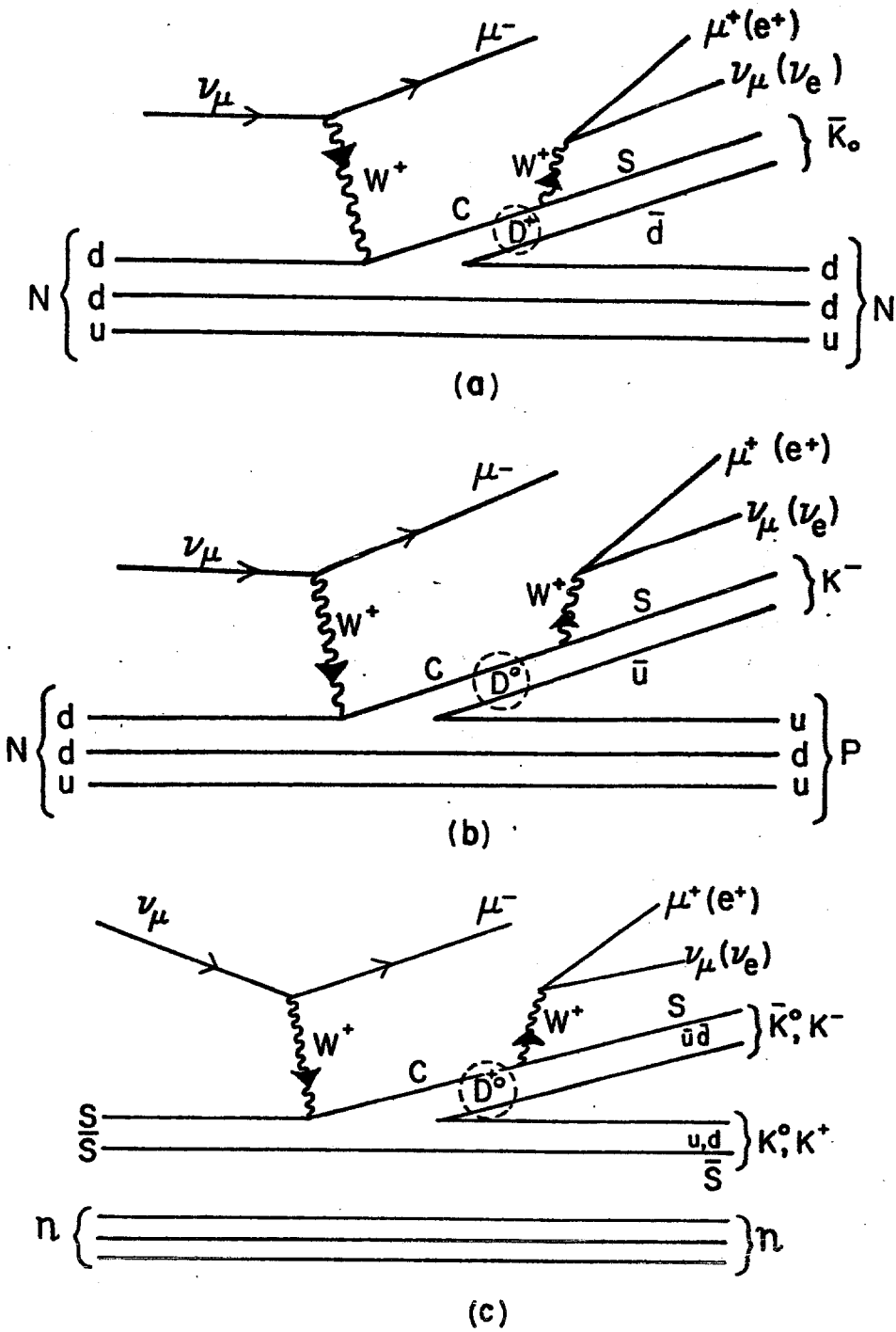


Figure 4

Quark diagrams for dileptons via charm production of D^+ and D^0 off valence quarks (a) and (b) and sea quarks (c).

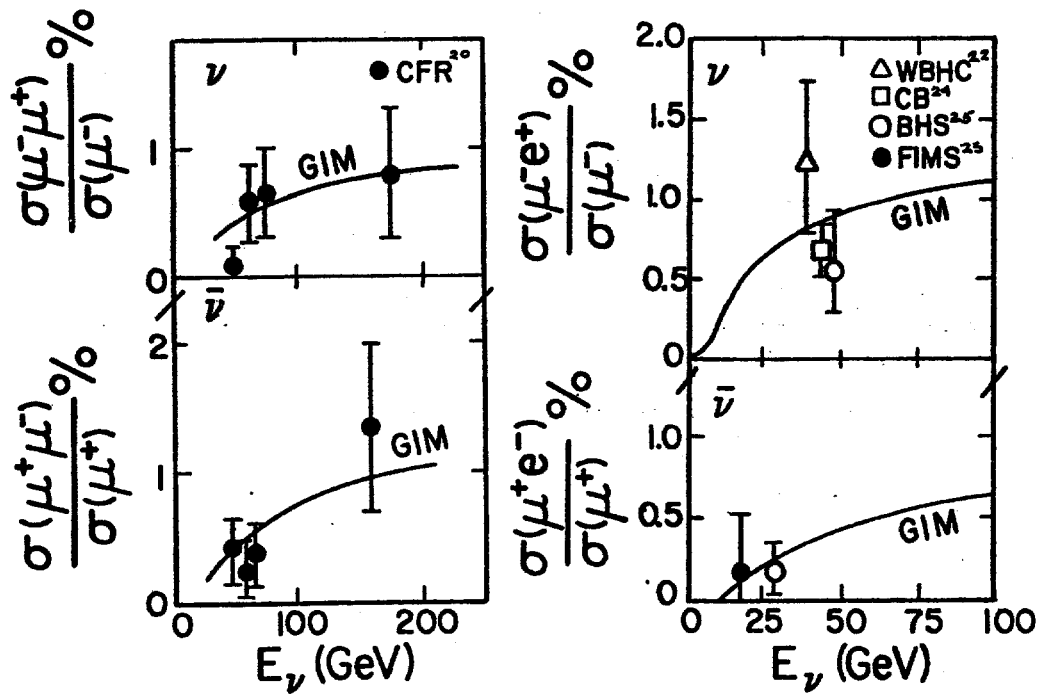


Figure 5

Relative yield of dilepton to single lepton events as a function of energy for $\mu\mu$ and μe final states for neutrinos and antineutrinos.

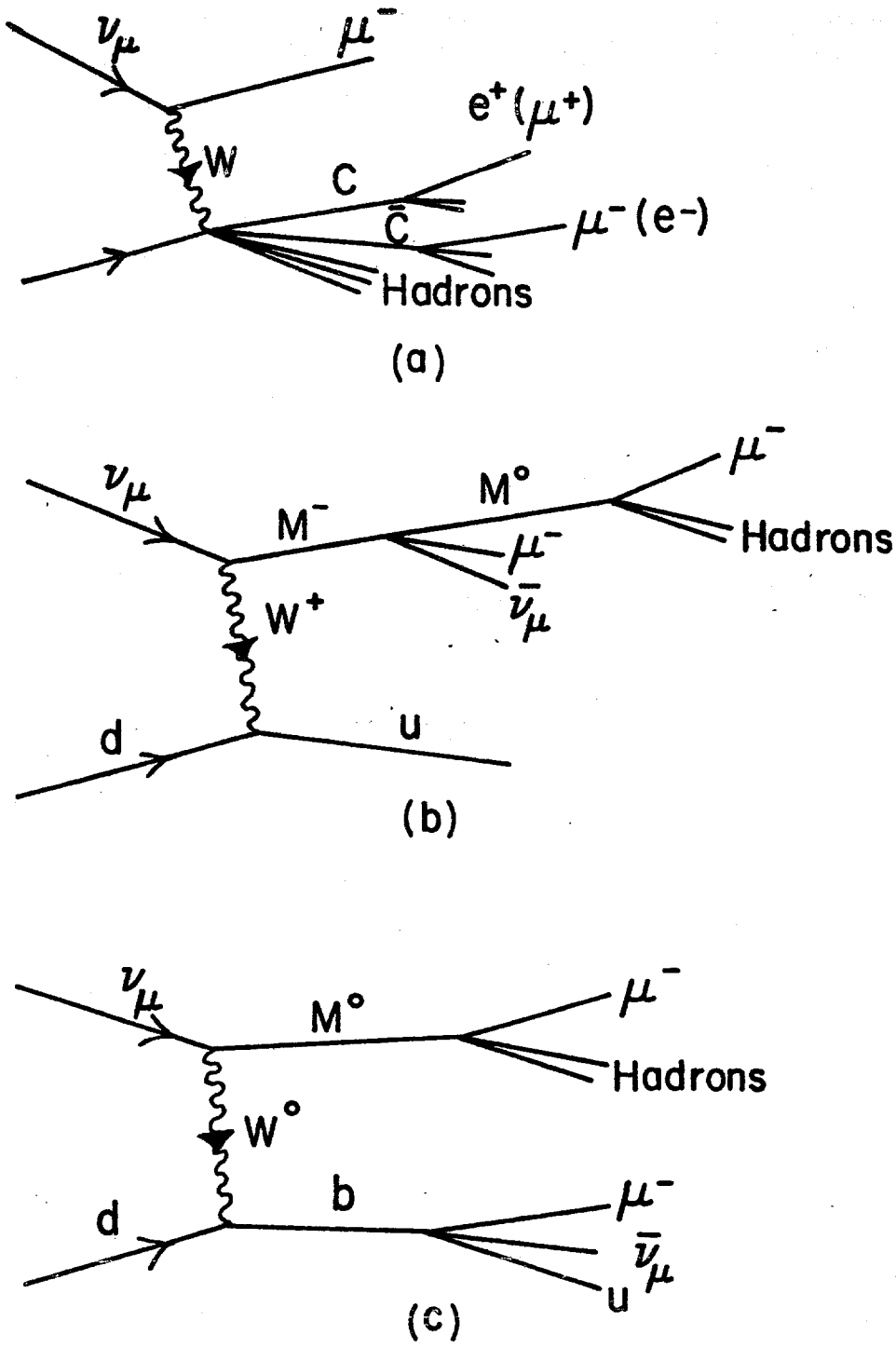


Figure 6

Same sign dimuon production from (a) charm-anticharm production at the hadronic vertex, (b) cascade decay of a charged heavy lepton and (c) decay of a bottom quark.

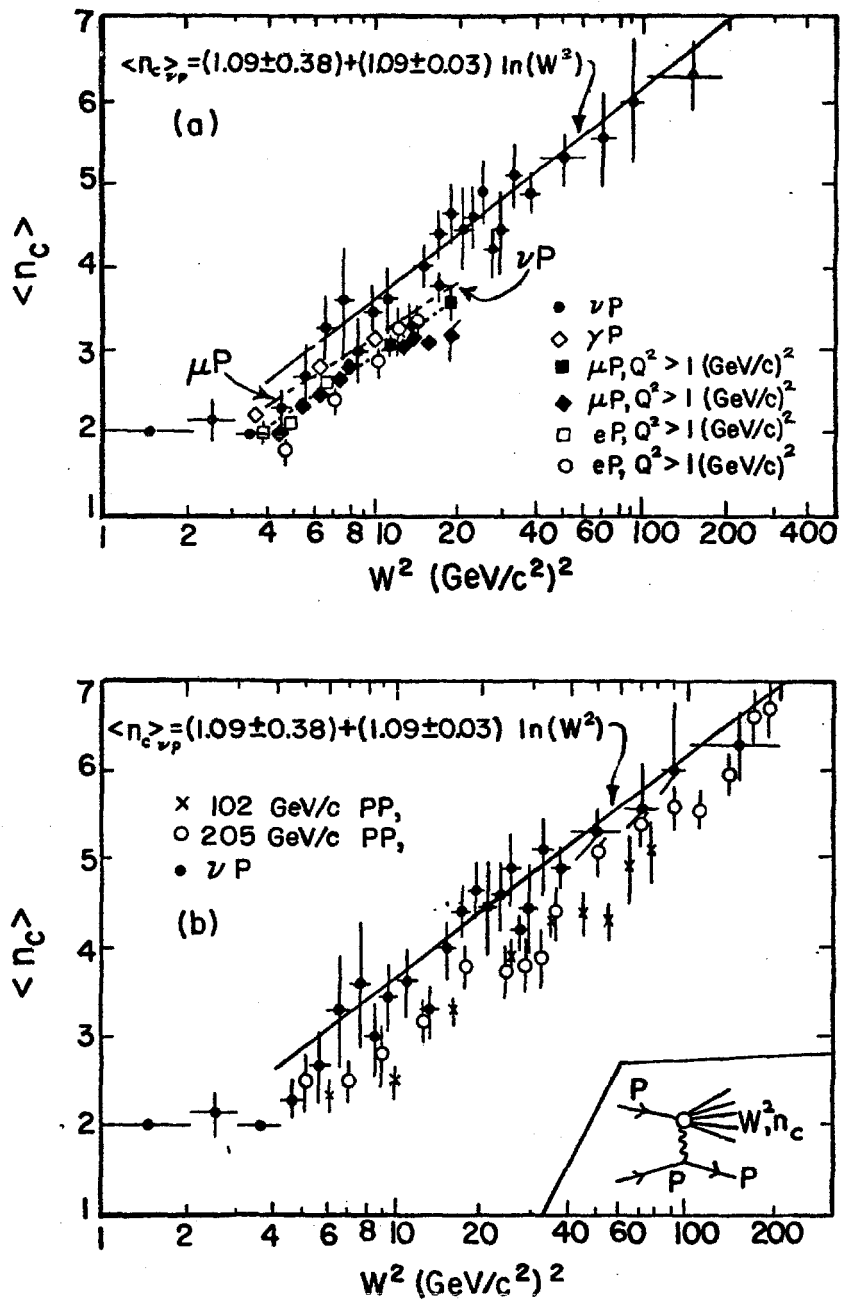


Figure 7

Comparison of mean charged-hadron multiplicity as a function of W^2 in νp scattering to that observed in (a) γp , $e p$, and μp interactions and in (b) inclusive pp scatterings. For references, see Ref. 35.

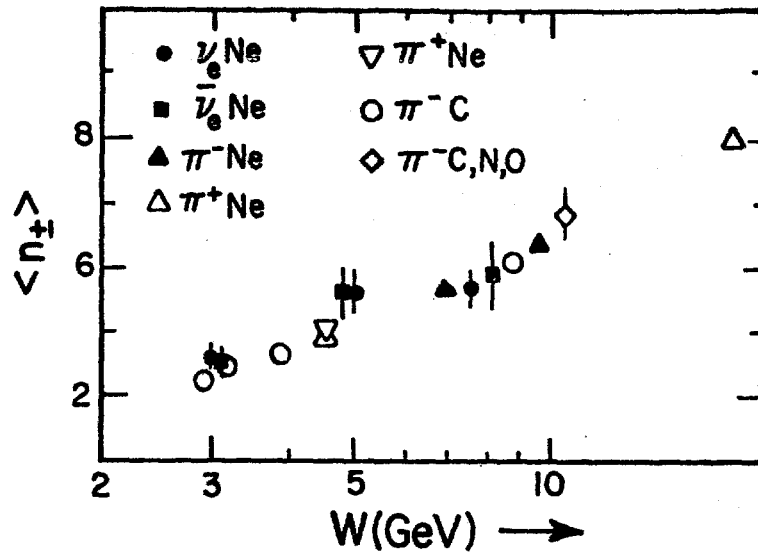


Figure 8

Comparison of mean charged hadron multiplicity as a function of W in ν_e -Ne and $\bar{\nu}_e$ -Ne scattering to that observed in pion interactions. For references, see Ref. 37.

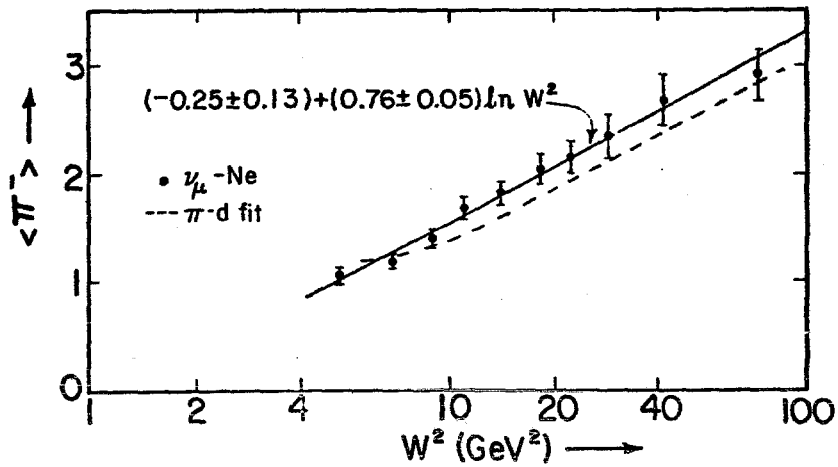


Figure 9

Comparison of the mean π^- multiplicity in $\bar{\nu}$ -Ne interactions with π^- d interactions.

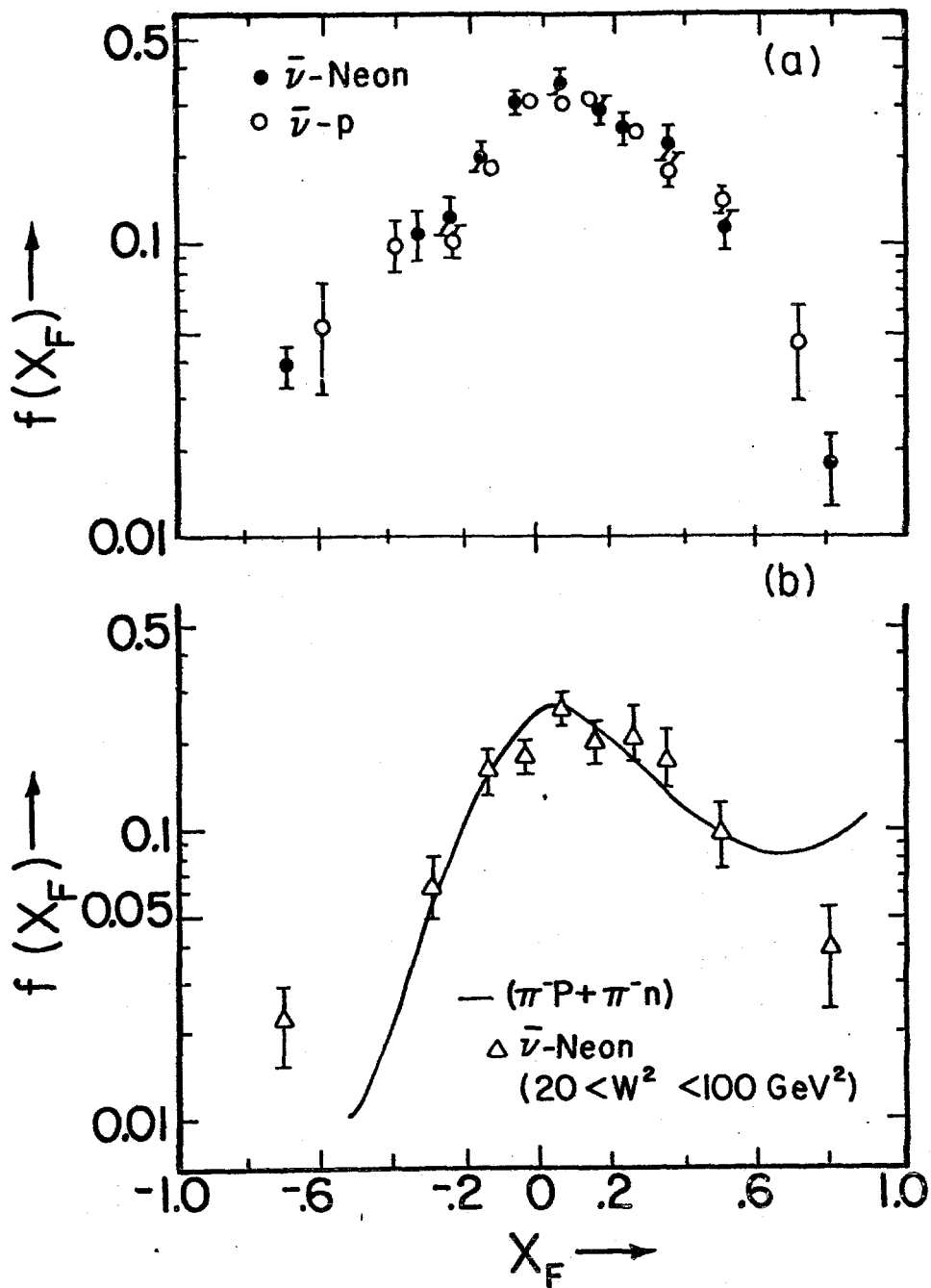


Figure 10

Comparison of the invariant yield $f(x_F)$ of π^- from $\bar{\nu}$ -Neon interactions as a function of Feynman x with (a) $\bar{\nu}$ -Proton interactions in the range $4 < W^2 < 100 \text{ GeV}^2$ and with (b) π^-p and π^-n interactions in the range $20 < W^2 < 100 \text{ GeV}^2$.

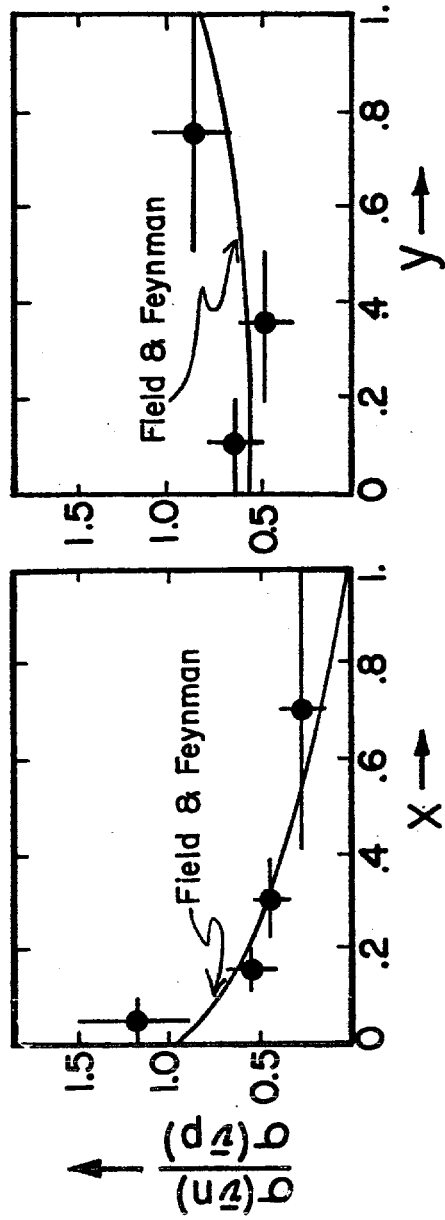


Figure 11

The relative yield of antineutrino-neutron to antineutrino-proton cross sections as a function of the scaling variables x and y. The solid curves are the predictions of Field and Feynman.

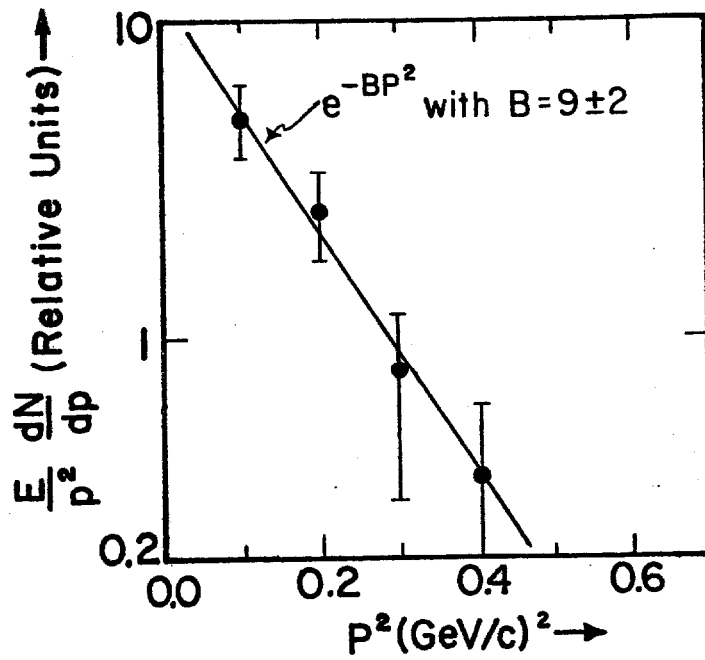


Figure 12

The momentum squared distribution for backward protons produced in $\bar{\nu}$ -Neon event. This distribution has been fit to the form e^{-BP^2} giving $B = 9 \pm 2$.

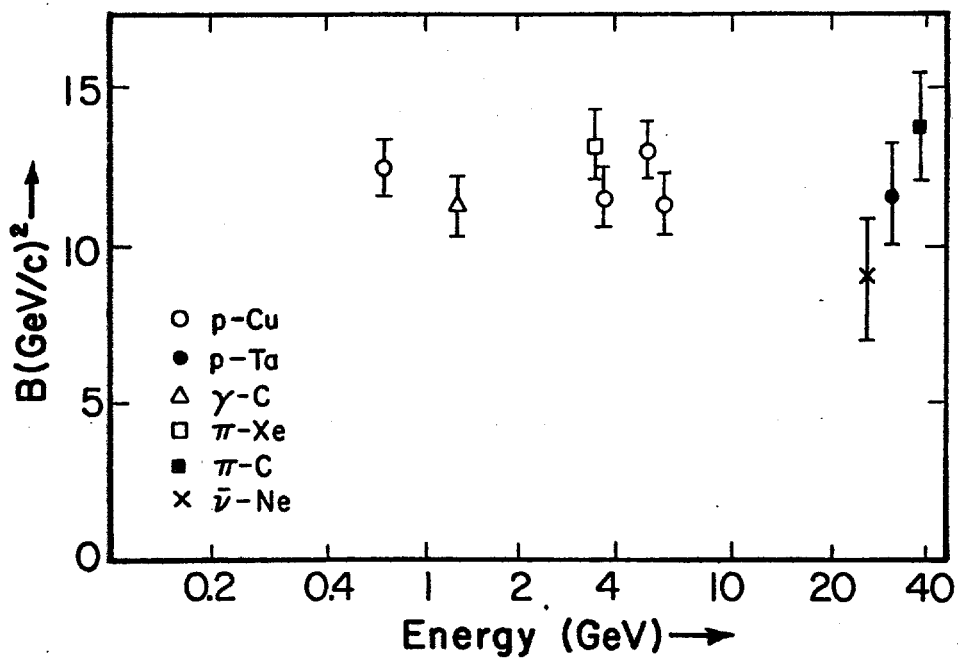


Figure 13

B values for backward proton momentum distributions produced in proton, gamma ray, pion and neutrino interactions. For references, see Ref. 46.

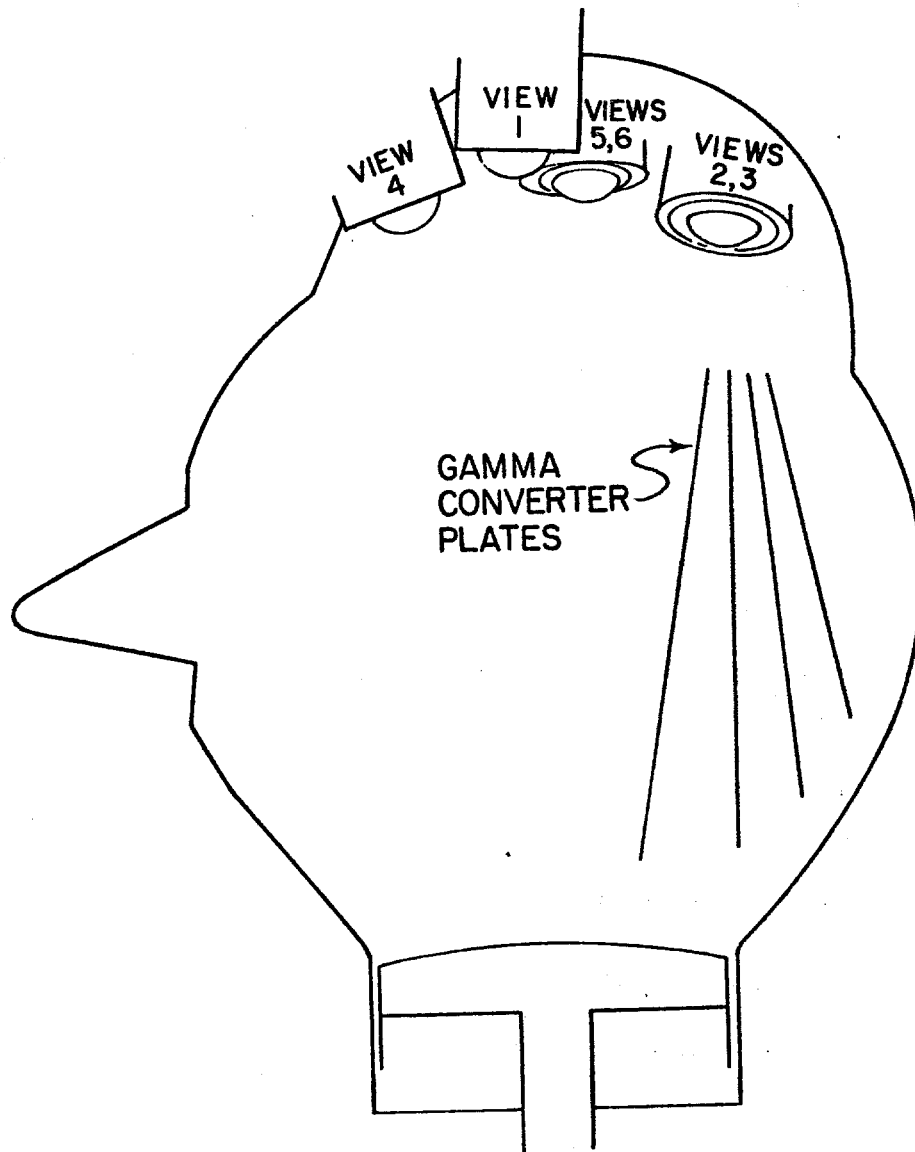


Figure 14

Pictorial representation of the 15-foot bubble chamber with gamma ray converter plates. The four plates are stainless steel, each one-half conversion length thick (~13 mm) and ~25 cm apart in the mid-plate.

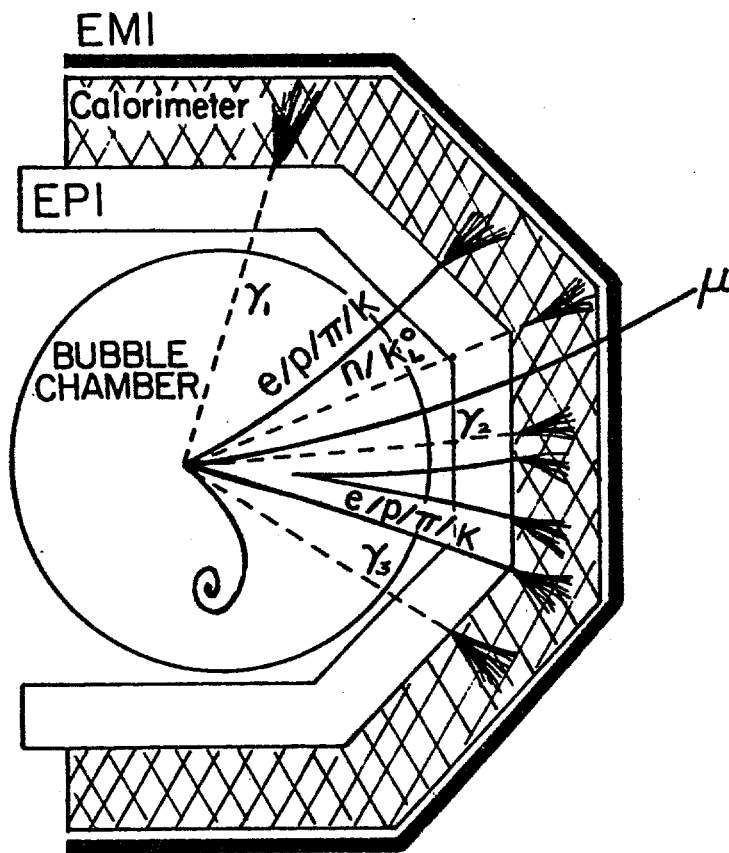


Figure 15

Hybrid bubble chamber for neutrino physics.

Bubble Chamber Provides:

- Target region for H_2 or D_2
- Magnetic field region
- Individual track measurements
- Λ and K_s^0 detection

EPI (External Particle Identifier) provides:

- Identification of charged track

Calorimeter provides:

- Identification and energy of electrons
- Detection and energy of neutral particles

EMI provides:

- Identification of muon